JOURNAL OF MECHANICS OF CONTINUA AND MATHEMATICAL SCIENCES
www.journalimcms.org

ISSN (Online): 2454 -7190, Vol.-20, No.-7, July (2025) pp 75-94 ISSN (Print) 0973-8975

DETERMINATION OF FRACTURE TOUGHNESS OF MILD STEEL UNDER MIXED-MODE CONDITIONS USING EXPERIMENTAL FINITE ELEMENT ANALYSIS

Anita Pritam[1], Peer Mohamed Appa M.A.Y.[2], S. Rahamat Basha[3], Bujjibabu Penumutchi[4], D. Naga Purnima[5], Ansari Faiyaz Ahmed[6], Yogesh Diliprao Sonawane[7], Chandrabhanu Malla[8], Rabinarayan Sethi[9]

[1]Mechanical Engineering, Odisha University of Technology and Research, Bhubaneswar, Odisha, India.

[2]Department of Artificial Intelligence and Machine Learning, School of Computing, Vel Tech Rangarajan Dr. Sagunthala R&D Institute of Science and Technology, Tamil Nadu, India.

[3]Department of Computer Science and Engineering, Malla Reddy College of Engineering and Technology, Hyderabad, Telangana, India.

[4]Department of Electronics and Communication Engineering, Aditya University, Surampalem, India.

[5]Department of Freshman Engineering, Aditya University, Surampalem, Kakinada, India.

[6]Department of Mechanical Engineering, University of Technology and Applied Sciences – Salalah, Dhofar, Oman.

[7]Assistant Professor, Department of Mechanical Engineering, Shri Vile Parle Kelavani Mandal's Institute Of Technology, Dhule, Maharashtra, India.

[8]Department of Mechanical Engineering, Radhakrishna Institute of Technology and Engineering, Bhubaneswar, Odisha, India.

[9]Mechanical Engineering, Indira Gandhi Institute of Technology, Dhenkanal, Odisha, India.

Email: [1]anitapritam@gmail.com, [2]peer.appa@gmail.com, [3]basha.ste@gmail.com
[4]bujjibabu_penumuchi@adityauniversity.in, [5]munukutla1977@gmail.com
[6]ansari.ansari@utas.edu.om, [7]yogeshsonaw@gmail.com
[8]chandrabhanu.malla@gmail.com, [9]rabinsethi@gmail.com

Corresponding Author: **Peer Mohamed Appa M.A.Y.**

https://doi.org/10.26782/jmcms.2025.07.00005

(Received: April 07, 2025; Revised: June 21, 2025; Accepted: July 05, 2025)

Abstract

This paper explores the fracture toughness of mild steel through experimental and finite element mixed-mode loading modeling. The experiment set the plate of size *rectangular of a through-edge inclined crack to find out the critical stress. The experimental results were then applied as input for modeling the specimen in ANSYS, where both the Mode I and Mode II stress intensity factors were computed. The hoop stress approach obtained the maximum hoop stress theory by use of which the critical stress intensity factor is calculated, which shows the fracture toughness of the material. These showed that the mild steel fracture toughness was between 53 and 78 MPa/m1/2. An experimental parametric study of crack length as well as crack inclination on stress intensity factors was carried out, giving insightful conclusions regarding material behavior in fracture in mixed-mode conditions.*

Keywords: ANSYS, Critical Stress Intensity Factor, Finite Element Method, Fracture Toughness, SIF.

I. Introduction

The integrity of engineering components is critical for the safety and reliability of various industrial applications, such as motor vehicle parts, oil and gas pressure vessels, pipelines, and welded joints. Such parts are exposed to complex loading conditions, a condition that results in the development and growth of cracks, which are key causes of structural failure [I]. Further fracture mechanics, the science of understanding the behaviour of cracked materials, is essential in understanding failure mechanisms. During World War II, many failures occurred in oil tankers and ships, which, under conventional design methodologies, had been expected to last longer. It was later determined that these failures were predominantly due to crack nucleation and propagation, which occurred at much lower stress levels than anticipated by the design specifications. This realization emphasized the need to better understand the fracture behaviour of materials under various loading conditions. Since then, fracture mechanics has become a central field of research aimed at predicting the failure of materials based on their fracture toughness, particularly under mixed-mode loading conditions where both opening (Mode I) and sliding (Mode II) cracks contribute to failure. Materials subjected to mixed-mode loading, where both tensile and shear stresses act simultaneously on a crack, exhibit more complex fracture behaviour compared to pure mode loading. The determination of fracture toughness under mixed-mode conditions is critical for accurately predicting the failure of materials used in engineering applications. The fracture toughness of a material may also depend upon factors such as the crack length, specimen geometry, the nature of loading (static or dynamic), residual stresses, loading rate, and the environment in terms of temperature, corrosion, and humidity. Thus, when looking at the fracture toughness of materials in mixed-mode conditions, it is necessary to consider these variables. Numerous studies have been devoted to the identification of fracture toughness of different materials in a mixed-mode setting, both through experiments and numerical procedures. Sietl et al. [II] examined the effect of out-of-plane and in-plane restrictions on the stress intensity factor and fracture toughness of the broken Al2024 specimen. The significance of such restrictions in measuring the resistance of the material to crack growth according to the mixed-mode loading was outlined in their work. Likewise, Li et al. [III] tested in Al2024 the orientation of the bifurcation of the fracture when the stress plan was combined. In their study, they have found that the J-integral value, which plays a vital role in crack propagation, significantly rises with loading angle and an increase in the influence of the second fracture pattern. More studies have been done to understand the influence of the material constitution on the fracture strength in mixed-mode fractures. In another study on the effect of manganese concentration on the fracture strength of Al2024 subjected to mixed-mode loading, the result of the study indicated that increasing the level of manganese improved the resistance to crack extension of the material to mixed-mode loading [IV]. In an investigation of the fracture behavior of ferrite steel under mixed-mode loading, Pirondi and Donne have also shown that the fracture toughness was lower as the loading angle became greater, but the crack tip migration vector was comparably little affected. A study of the influence of specimen thickness on mixed-mode fracture toughness has also been used [V]. Zhang et al. examined the influences of specimen thickness and high temperatures on the fracture toughness of titanium in mixed modes [VI]. They found that the thickness had a great effect on the crack propagation (fracture toughness), particularly at high temperatures. Guo et al. investigated the fracture properties of LC4-CS aluminum alloys through mixed-mode I/II loading and found that the first mode loading load capacity decreased with the increasing specimen thickness, but the mixed-mode loading did not show a significant difference in the thickness [VII]. Pearce et al. looked into the importance of loading angle and failure force in mixed-mode fracture behaviour, where they experimented on bolted composite components using a modified Arcan test rig. They found that when the loading angle was increased, there was a decrease in failure force, which meant that it decreased the fracture toughness when there was a mixed-mode loading [VIII]. The influence of loading mode on fracture toughness was also investigated by Fagerholt et al., where they came to find that Mode I loading led to higher peak loads than Mode II and mixed-mode loading [IX]. Mixed-mode loading of materials has been popularly examined by numerical simulations to learn about the fracture behaviour of materials. Matvienko et al. conducted a numerical study of the effect of thickness changes on stress intensity factors subjected to a mixed-mode I/II loading and focused on the contribution of T-stresses and the significance of mode mixity [X]. Even at the mixed-mode crack formation in the semicircular bend samples, Aliha and Saghafi conducted a comparative study of two-dimensional and three-dimensional simulation methods and concluded that 3D models all give better results compared to the 2D ones [XI]. In finding the load-bearing capability and the angle of fracture initiation in the notched specimens, Nasrnita and Aboutalebi revealed that the use of stress-based finite element analysis proved superior to the use of strain in these findings [XII]. In the current research work, a mixture of both experimental and finite element methods is used to ascertain the fracture toughness of mild steel subjected to mixed-mode [XIII]. Experimental testing was done on a flat plate with a crack inclined on an edge that had the dimensions in the form of a rectangle to establish the critical stress [XIV]. A finite element model of ANSYS was then represented using experimental data to determine the stress intensity factors of both Mode I and Mode II loading conditions. To look into the effect of the crack length and inclination on the stress intensity factor, a parametric study was also carried out [XV-XIX]. The purpose of this study is to present a more in-depth picture of the fracture behaviour of mild steel in mixed-mode loading modes, which is critical in enhancing the safety of the design and safety of engineering components during complex environmental loading [XX-XXV].

II. Experimental Study

This research paper was conducted through experiments and calculations to ascertain the fracture toughness of mild steel at mixed-mode loading conditions. At the beginning, a mild steel specimen containing an inclined crack was produced, and experiments were made to determine critical stress values of various crack lengths and angles (45° and 60°). The lengths of the cracks were manipulated to check their effects on the stress intensity factor. The experimental results such as critical stress values were then applied to carry out Finite Element Method (FEM) analyses in ANSYS where the stress intensity factors (Mode I, tensile as well as Mode II, shear) were calculated. The experimental data were compared with the outcome of the numerical simulations to find the accuracy of the method of calculations. They also conducted parametric studies to determine the argument of how crack length and crack angle affect the stress intensity factor to gain some understanding of the mixed-mode fracture toughness of mild steel.

Experiments to determine critical stress

The experiment was done to measure the critical stress intensity factor of a mild steel sheet metal specimen of dimension 0.2x0.1x0.0015 m^3 of eighteen different specimens having different crack lengths and different angles of the crack. Fig. 1 and Fig. 2 show the specimens of different crack lengths at 45-degree and 60-degree crack orientations, respectively.

Fig. 1. Crack angle 45 degrees (a= 0.03, 0.035, 0.04m)

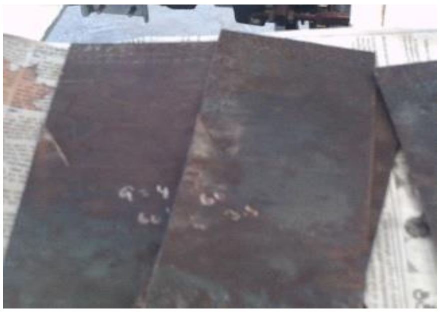

Fig. 2. Crack angle 60 degrees (a= 0.035, 0.04m)

Figure 1 illustrates the fracture behaviour of a mild steel specimen with an inclined crack at a 45-degree angle. The crack length is varied in three different values, specifically 0.03m, 0.035m, and 0.04m, to observe the influence of crack length on the stress intensity factor. The 45-degree crack angle is chosen to simulate a typical scenario where both tensile and shear stresses contribute to the crack propagation under mixed-mode loading conditions. The varying crack lengths provide insights into how the geometry of the crack impacts the material's fracture toughness under these loading conditions. Shorter cracks may experience lower stress intensity factors, while longer cracks typically result in higher stress intensity factors, making the material more susceptible to fracture. The impact of crack length on the stress intensity factor is significant as it determines the material’s resistance to crack propagation. The longer the crack is, the greater the stress intensity factor is, and when it reaches a sufficient length, it will propel the material to its critical stress and break. The stress intensity factor values of various lengths of the crack are applicable to know the performance of the materials under mixed-mode stress conditions, which proves to be crucial in such cases, such as pressure vessels, pipelines, or welded joint applications, when the crack length is variable. The behaviour of the fracture of a mild steel specimen, having a crack inclined at a 60-degree angle, is illustrated in Figure 2. Here, the lengths of the cracks taken among the test sample are 0.035m and 0.04m to test the effect of crack length on the fracture toughness at a different angle of inclination. The angle of the crack, which is at 60 degrees, will be steeper than the angle at 45 degrees, and it will exhibit varying interactions of tensile and shear stresses at the crack tip. The experimental findings are quite useful in determining the effects of crack angles on the mixed-mode fracture toughness of materials under study. The crack has a higher ratio of shear stress (Mode II) at a 60-degree angle of crack than at a 45-degree angle of crack, where there can be more tensile stress (Mode I). Alteration of loading conditions may influence the fracture behaviour of the material, and the consequent stress intensity factors assist in determining this influence. The effect of crack length on the resistance of the material to crack propagation was studied by examining two crack lengths 0.035m and 0.04m as observed in Figure 2, where it was apparent that crack length at a sharper angle had a significant effect on the resistance to crack propagation of the material [XX].

The stress intensity factor of the crack at the 60-degree angle rises as the crack length rises, and this also helps in comprehending the effect of crack geometry on the mixed-mode fracture toughness. When comparing the data given by Figures 1 and 2, it is possible to note that the crack angle has a quite notable influence on the fracture toughness of the mild steel specimen. At 45 degrees (Figure 1), there is an equivalent influence of Mode I (opening) and Mode II (sliding) stresses on the material, and therefore a response of lower fracture toughness at 45 degree crack rotation than that of the 60 degree (Figure 2). The increase in shear component by the 60-degree crack angle tends to cause an increase in the stress intensity factor, and on some occasions, it may reduce the overall fracture toughness. This emphasizes the significance of the crack angle in the analysis of mixed-mode fracture as the ratio between tensile and shear strength is essential to the fracture behaviour of the material, as shown in both figures, the increase in the length of the crack in most cases will increase the stress intensity factor but the rate of change may vary between both angles. This plays a very significant role when engineering parts experience a multifactorial load state, since the information provided allows the engineer to make better predictions on cracking. The type of crack angles and lengths not only helps to give a vast description of the fracture mechanics of mild steel, but also one that can be applied in real engineering problems since it guarantees a dependable and safer design. The findings of the two figures are of great significance in engineering, where materials have to be loaded in the mixed mode, i.e., pressure vessels, bridges, or aircraft structures. The knowledge of how crack length and crack angle affect the fracture toughness enables a better prediction of the behavior of materials in the case of stress. This will assist engineers when they design parts that are more likely to resist failures, especially in such a case where we may have the creation of cracks that could extend and result in failure. These figures, together with their experimental and numerical analysis, provide useful information on how to enhance the durability as well as the safety of this critical infrastructure.

Experimental Set Up

There are two important apparatuses in the preparation of the experiments to ascertain the fracture toughness of the mild steel, and they include the Universal Testing Machine (UTM) and the shearing machine. The tests could not have been conducted without these machines or be able to prepare the specimen to carry out the tests to determine the fracture toughness under mixed- modes. Machinery was used in different roles, either during the specimen preparation or in the actual test, such that the critical load and stress intensity factors were established. Critical load of the specimens was measured using the UTM, which has a load of 40 tons. The UTM is divided into two major subsystems, that is, the control unit and the testing unit. The testing unit involves the testing of the specimen between two cross-heads, which are lower and upper, held by the control unit that enables the control of the needs of the testing procedure. The specimens, which had different crack lengths and angles, in this study, were exposed to a loading condition whereby the values of critical stress could be calculated. The UTM was essential in exerting controlled loads to the specimens and measuring the force necessary to cause a crack to propagate, which is used to determine the fracture toughness. The specimens were cut into the desired size using the shearing machine to cut the sheet metal. It comprises different parts, such as a cutting lever, a handle, and a table where the metal sheets are placed to be cut. The precision required to precisely cut the sheet metal into eighteen different pieces of the dimensions of 0.2x0.1 m^2 was provided by the shearing machine, which was to aid in the fracture toughness tests. The advantage of the shearing machine in cutting assisted in obtaining uniformly cut specimens with a controlled dimension, so that the crack and geometries would be controlled accurately during the test. The preparation of specimens required some steps to make each specimen compatible and have the specifications necessary to experiment. First, they used the shearing machine to cut a very big piece of mild steel into eighteen pieces. The dimensions of each piece were 0.2 x 0.1 m, and each sheet of paper was also measured in thickness, whereby its accuracy was recorded using a digital Vernier caliper (0.0013 m). Following the fundamental atrocity, different angles and long cracks were incorporated into each sample, which was accomplished with a bevel protractor and steel rule. The crack orientations and lengths were maintained with precision using these tools, and they are important parameters in the process of determining fracture toughness. The cracks were thereafter introduced back into the samples in the shearing machine, ensuring that they were consistent with all the samples. After preparation of the specimens, they could be tested in the UTM. Specifications of the specimens are listed in detail in Table 1, and Figure 3 indicates the configuration of the specimens adopted in the experiments.

Table 1: Specimen Specification

Sl. No.	Linm	b in m	t in m	a in m	θ
1	0.200	0.100	0.0013	.030	30°
2	0.200	0.100	0.0013	.032	30°
3	0.200	0.100	0.0013	.035	30°
4	0.200	0.100	0.0013	.037	30°
5	0.200	0.100	0.0013	.040	30°
6	0.200	0.100	0.0013	.042	30°
7	0.200	0.100	0.0013	.030	45°
8	0.200	0.100	0.0013	.032	45°
9	0.200	0.100	0.0013	.035	45°
10	0.200	0.100	0.0013	.037	45°
11	0.200	0.100	0.0013	.040	45°
12	0.200	0.100	0.0013	.042	45°
13	0.200	0.100	0.0013	.030	60°
14	0.200	0.100	0.0013	.032	60°
15	0.200	0.100	0.0013	.035	60°
16	0.200	0.100	0.0013	.037	60°
17	0.200	0.100	0.0013	.040	60°
18	0.200	0.100	0.0013	.042	60°

where L= length of job-piece, b= width of job-piece, t= thickness of job-piece, a= crack length, **θ**= angle of crack.

Table 1 contains the specifications of the specimens to be used to find out the fracture toughness of mild steel under mixed-mode conditions. The individual specimen all possesses certain dimensions and crack properties which have been varied to determine the influence of crack length and orientation on fracturing behaviour. The measured parameters in the table were the length (L), width (b), thickness (t), crack length (a), and the crack angle (0). The length (0.200 m), the width (0.100 m), and the thickness (0.0013 m) of all of the specimens were equal, providing similarity in total geometry. The first variable was crack length (a), and the second one was crack angle (0), which was systematically varied between the specimens. The crack dimensions varied between 0.030 m and 0.042 m, and the crack angle (θ) was fixed in three positions, namely 30°, 45° and 60°. These variations were aimed at observing the effect of a change in crack shapes on the material's fracture toughness. The specimen geometry involving differences in crack lengths and directions will help examine the behaviour of the material under mixed-mode loading in great detail. Such a variety of crack angles (30° to 60°) is an important aspect since the realistic loading conditions in engineering structures are inclined cracks. It is hoped that through these different specimens, the study will further understand the relationship that exists between crack geometry and fracture toughness; a useful information that can be used to understand how the material can respond to various stress conditions.

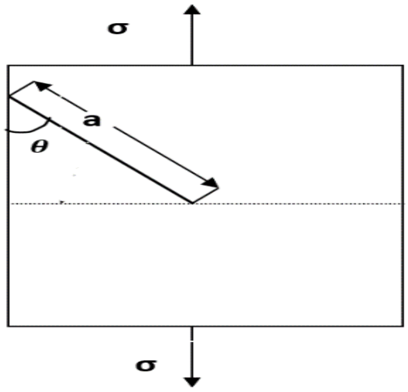

Fig. 3. Specimen Configuration

The sample geometry of the specimens in the fracture toughness tests is pictorially shown in Figure 3. Its specimens were in the form of a rectangle with regular length (0.200 m), width (0.100 m), and thickness (0.0013 m). Each specimen was subjected to the introduction of a crack of different length (0.030 m to 0.042 m) and introductions at various angles (30, 45, and 60. The crack was strategically located on the wide side of the specimen and initiated at one end, just like they would naturally occur in the field. The accurate placement and measurement of the crack is necessary to analyze the precise determination of the fracture toughness under the mixed-mode. In geometry and location, the figure probably emphasizes the size and location of the crack compared with the size of the entire specimen, and this gives a graphical impression of how the geometry affects fracture behaviour. The crack angle (θ) is of vital essence because it helps in calculating the stress intensity factors in a mixed-mode loading condition, since the stress distribution around the crack face is influenced by crack orientation. This experimental configuration will enable us to analyze the effect of crack length and angle comprehensively to examine the effect they have on the fracture toughness of mild steel in different loading conditions.

Experimental Procedure

To determine the fracture toughness of the specimen, we have used a 40-ton UTM (Universal Testing Machine). Following the specimen preparation, it was taken to the UTM to be tensile tested. The specimen was mounted between the lower and the upper cross-head of the UTM, and subsequently, loads were applied to the specimen. Then the load at which the crack started propagating was read on the dial indicator of the UTM in each specimen. They had recorded the loads at each specimen where the crack was initiating its propagation. The critical stress was calculated by dividing the critical load by the area. Table 2 shows the data for critical loads for different crack lengths and angles.

Table 2: Data of critical loads at various crack lengths and crack angles

Crack length, a(m)	θ = 30°	θ = 45°	θ = 60°
	Load (N)	Load (N)	Load (N)
0.03	20601	23053.5	30411
0.032	19659.2	22759.2	26487
0.035	17658	21582	23544
0.037	15931.4	20306.7	24346
0.04	12753	17658	26487
0.042	10241.6	15401.7	30212

Table 2 provides the data on critical loads measured for specimens with varying crack lengths (a) and crack angles (θ). The table presents the critical load values (in Newtons) required to cause failure for three different crack angles: 30°, 45°, and 60°. For each crack length, the load values are recorded across the three crack angles, reflecting how the orientation of the crack influences the material's resistance to fracture. The crack lengths range from 0.030 m to 0.042 m, and the corresponding critical loads indicate the strength of the material under different loading conditions. Based on the results, it is noted that the critical load at which a fracture is initiated tends to decrease as the crack length is increased at all crack angles. For instance, at a crack length of 0.03 m, the critical loads are highest, with values of 20601 N for θ = 30°, 23053.5 N for θ = 45°, and 30411 N for θ = 60°. As the crack length increases, the load values gradually decrease, with the lowest critical loads observed at a crack length of 0.042 m. This trend suggests that larger cracks weaken the material, requiring less load to cause failure. From the table, it is clear that the critical load is achieved. For example, at the smallest crack length (0.03 m), the critical load is highest for a crack angle of 60° (30411 N) and lowest for a crack angle of 30° (20601 N). This pattern continues across different crack lengths, with 60° crack angles consistently requiring higher loads to cause fracture compared to the other angles. This suggests that the crack angle influences the stress distribution at the crack tip and, consequently, the material's fracture toughness.

III. Finite Element Model Development

The material that was employed during the experiment, the same was modeled in ANSYS. Making key points, lines, and areas involves the following steps, done in the preprocessor during modeling. There was no gap in the modeling of the crack (fine slit). That was achieved through the creation of a two-line merge between them. In this analysis, the property of the material was fixed to be that of mild steel. The Youngs modulus and the Poisson ratio are provided as 210 GPa and 0.3, respectively. The bottom of the model is bound on the X and Y axes. Through the upper line, the net pressure was imposed in the upward direction. We obtained the value of pressure as a result of our experiment. ANSYS is used to carry out linear static Finite element analysis to extract stress and displacement at various points of the model. However, in this case, the target was to acquire SIF. Path operation is performed by choosing five nodes beginning at the crack tip to get the SIF. Once more, a local coordinate is defined at the crack tip, wherein the stress value in the exterior surroundings is extrapolated to the crack tip. Finally, due to the KACLC command, mode-I and mode-II stress intensity factors are to be obtained. Table 3 provides the results obtained in terms of stress intensity factors associated with Mode I and Mode II failures with the help of the Finite element method. ANSYS is the source of these data.

According to the maximum circumferential, or hoop, stress theory, a fracture will propagate along the orientation of maximum hoop stress, when $\sqrt{r}\sigma_{\theta\theta}(r, \theta) \geq$ Const. Considering that, the constants are equal for mixed-mode loading as for pure Mode-I loading where KI ≥ Kic, the mixed-mode formula may be written as:

$$\sqrt{r}\sigma_{\theta\theta}(r,\theta) \geq \frac{Kic}{\sqrt{2\pi}} \tag{1}$$

The directional principle is that the crack will extend in the direction θ, which gives:

$$\frac{\partial \sigma_{\theta\theta}}{\partial \theta} = 0 \tag{2}$$

$$\sigma_{\theta\theta}(r,\theta) = \frac{1}{\sqrt{2\pi r}}\left(K1\cos\frac{1+\cos\theta}{2} - K11\frac{3}{2}\sin\theta\cos\frac{\theta}{2}\right) \tag{3}$$

Table 3. Stress intensity factor for mode I and mode II

Θ (in degrees)	a (m)	KI	KII
30	0.03	66.91	21.58
	0.032	68.33	22.02
	0.035	67.95	21.64
	0.037	65.31	20.69
	0.04	58.07	18.22
	0.042	51.07	15.88
45	0.03	52.49	26.52
	0.032	55.13	27.76
	0.035	56.82	28.47
	0.037	56.43	28.17
	0.04	53.56	26.57
	0.042	50.13	24.73
60	0.03	41.2	29.49
	0.032	37.32	26.69
	0.035	35.87	25.58
	0.037	37.83	26.91
	0.04	45.12	32.01
	0.42	52.9	37.48

Solution of equations 1,2, and 3 gives the angle of crack extension θ_0

$$\tan\frac{\theta_0}{2}=\frac{1}{4}\frac{K1}{K11}\pm\frac{1}{4}\sqrt{\left(\frac{K1}{K11}\right)^2+8} \tag{4}$$

$$\sigma_\theta=\frac{K1}{\sqrt{2\pi r}}\cos\frac{\theta_0}{2}\left(1-\sin^2\frac{\theta_0}{2}\right)+\frac{K11}{\sqrt{2\pi r}}\left(-\frac{3}{4}\sin\frac{\theta_0}{2}-\frac{3}{4}\sin\frac{3\theta_0}{2}\right) \tag{5}$$

The maximal circumferential tensile stress,σ_{θ}, that is calculated by modifying equations 4 and 5, must approach a critical level for the crack to propagate.

$$\sigma_{\theta\max}\sqrt{2\pi r}=Kic=\cos\frac{\theta_0}{2}\left[K1\cos^2\frac{\theta_0}{2}-\frac{3}{2}K11\sin\theta_0\right] \tag{6}$$

which can be normalized as:

$$\frac{K1}{Kic}\cos^3\frac{\theta_0}{2}-\frac{3}{2}\frac{K11}{Kic}\cos\frac{\theta_0}{2}\sin\theta_0=1 \tag{7}$$

These equations 6, 7, and 8 can be utilized to define an analogous stress intensity factor (critical stress intensity factor) Kic for mixed-mode Problems

$$Kic=K1\cos^3\frac{\theta_0}{2}-\frac{3}{2}K11\cos\frac{\theta_0}{2}\sin\theta_0 \tag{8}$$

Table 4 indicates the level of fracture toughness (critical stress intensity factor): different crack lengths as well as different crack angles.

Table 4: Value of fracture toughness (Kic) for different crack lengths

ϴ (in degrees)	a (m)	KI	KII	Kic
30	0.03	66.91	21.58	75.94
	0.032	68.33	22.02	77.54
	0.035	67.95	21.64	76.92
	0.037	65.31	20.69	73.85
	0.04	58.07	18.22	65.54
	0.042	51.07	15.88	57.53
45	0.03	52.49	26.52	67.58
	0.032	55.13	27.76	70.68
	0.035	56.82	28.47	72.95
	0.037	56.43	28.17	72.11
	0.04	53.56	26.57	68.52
	0.042	50.13	24.73	63.77
60	0.03	41.2	29.49	61.49
	0.032	37.32	26.69	54.27
	0.035	35.87	25.58	53.41
	0.037	37.83	26.91	54.85
	0.04	45.12	32.01	67.01
	0.42	52.9	37.48	76.53

Table 4 presents the fracture toughness (Kic) values calculated for different crack lengths (a) at various crack angles (θ). The table shows the stress intensity factors KI (Mode I) and KII (Mode II) along with the resulting fracture toughness (Kic) for each combination of crack length and crack angle. KI and KII represent the contributions from the opening mode and sliding mode of crack propagation, respectively. Kic is the critical fracture toughness, which is the point at which the material is expected to fracture under the applied load. For each crack length, as the crack angle increases, the Kic values tend to decrease, showing a decreasing trend in material toughness as the crack angle shifts from 30° to 60°. At a crack angle of 30°, the fracture toughness values range from 75.94 MPa√m (for a = 0.03 m) to 57.53 MPa√m (for a = 0.042 m). The findings show that with longer crack length, the fracture toughness diminishes, confirming the previous findings since the longer crack size prompts a decrease in the material's immunity to fracture. The same trend is noticed at other crack angles, whereby the fracture toughness also becomes lower with an increase in crack length, although a different rate of decrease is noticed at different crack angles. For example, at θ = 45°, the fracture toughness ranges from 67.58 MPa√m (for a = 0.03 m) to 63.77 MPa√m (for a = 0.042 m), showing a similar decreasing pattern as the crack length increases. The results for θ = 60° reveal that the fracture toughness values are comparatively lower than those for the 30° and 45° crack angles, indicating that a higher crack angle leads to a reduction in fracture toughness. For example, at a crack length of 0.03 m, the fracture toughness is 61.49 MPa√m, which decreases significantly to 54.27 MPa√m for a crack length of 0.032 m. However, at larger crack lengths (0.04 m and 0.042 m), the fracture toughness increases again, peaking at 76.53 MPa√m for a crack length of 0.042 m. This behavior suggests that while the crack angle influences the toughness, the crack length is a more significant factor in determining the fracture toughness of the material.

III. Results and Discussion

Variation in stress intensity factor

The phenomenon used in fracture mechanics to determine the state of stress adjacent to the crack tip is the stress intensity factor. The punchline is that stress at the crack tip, according to linear theory, is infinite, but in actuality, there is a plastic region at the crack tip, and hence, stresses remain finite. The size and location of the crack, the size of the load distributions on the specimens, all lead to the value of SIF. The SIF can be regarded as a parameter that increases the stress being applied. In this section, the graphs of the results received to represent SIF in mode I and mode II have been shown and discussed herein. The numbers (4) are the variations of SIF against crack length at different orientations of cracks. The SIF variation with variations in orientations is found to act in different ways. Considering the 30-degree crack orientation model, which is diagrammatically represented by Fig. 4a, it is possible to note that when the length of the crack varies by 30mm-35mm, there is an insignificant rise in values of KI and KII. Mode I: The mode I fracture rate of occurrence seems to be greater than mode II fractures. The reduction in SIF values in mode I and mode II is easy to be observed when the crack is larger than 35 mm. The phenomenon of stable crack growth region distribution can be regarded as the source of lowering the SIF. It has also been stated in the literature concerning fracture mechanics that there will be an increase in SIF with a range of 0a in which as we go beyond that range within which the SIF can be seen to decrease. Other hints by some authors that have been advanced include the induction of material non-linearity as an explanation for the drop in the values of SIF in some instances, especially at higher a/w ratios.

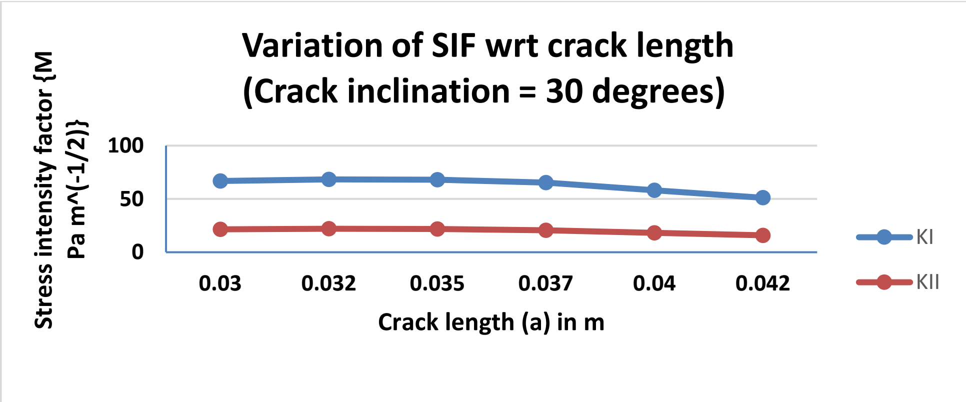

Fig. 4a. variation of SIF w.r.t. crack length at 30 degree

Figure 4a illustrates how the Stress Intensity Factor (SIF) changes with a crack length at the angle of 30°. The SIF is a very important fracture parameter employed by fracture mechanics to define the state of stress around the crack tip. It is a significant indicator of the resistance of the material to crack propagation. The length of the crack (a) is plotted on the x-axis in this plot, whereas the values of SIF, respectively (KI and KII), are plotted on the y-axis. It can be noted on the graph that as the lengths of the cracks lengthen, the value of the KI (Mode I) and KII (Mode II) also rises. This is normal because larger cracks offer a greater crack area to which tension can become concentrated, thus heightening the level of the stress field at the crack tip. In particular, KI (Mode I) shows a much larger increase as compared to KII (Mode II), which reveals that the opening mode (tensile stress) of the crack plays a leading role in crack propagation at a 30 o crack angle. This attribute is indicated by the magnification of KI at longer crack length, which implies that the longer the crack gets, the more tensile stresses are exerted on the material, which becomes more prone to a crack. This graph shows a relatively straight correlation between the crack length and SIF at the lower crack lengths, followed by a slight flattening out at the longer crack lengths. This is an indication that at some point, the crack will be at a stage where the stress intensity increase is at a slower rate, possibly because the material is naturally resistant to further crack growth or the alteration in the geometry of the crack tip. In general, the figure demonstrates the paramount importance of the crack length in the calculation of the stress intensity factors and, therefore, fracture toughness of the material when loaded with mixed-mode loading.

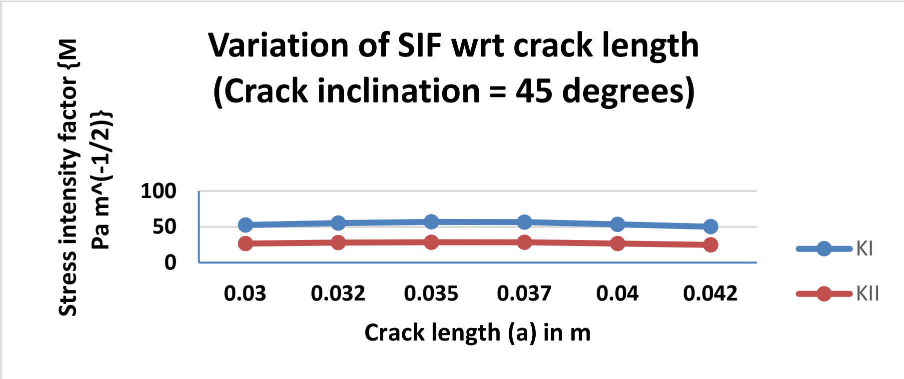

Fig. 4b. variation of SIF w.r.t. crack length at 45 degree

Figure 4b shows the change of Stress Intensity Factor (SIF) to the crack length at the crack angle of 45^o. As in the case with the previous figure (Fig. 4a at 30^o), the x-axis is crack length (symbolized as a), and the y-axis is SIF values specific to both Mode I (KI) loading and Mode II (KII) loading conditions. In Figure 4b, we saw that as the crack length increases, both KI and KII increase as well. This tendency agrees with the fundamental features of fracture mechanics, according to which the longer the crack, the greater the stress concentration in the vicinity of the crack tip. At a crack angle of 45, the effect of SIF is higher than compared to a 30-degree angle-linear stiffness (KI). This implies that at 45, the material experiences a mixture of tensile stress and shear stress, and it is as the crack extends, the effect of shear stress (KII) is greater as compared to 30^o cases. The Fig. 4c represents the fluctuation in the SIF of the specimen of cracked orientation 60^o. The characteristics of the curve in this case are different. This investigation reveals that the SIF will reduce to a proximity of about 30-35mm crack length. Hence, the stable crack growth effect or the non-linearity of a material can be believed to have happened in the past. The SIF will likely rise in the range of 35-42mm crack length, thereby indicating that the stress values used will be amplified more at this range.

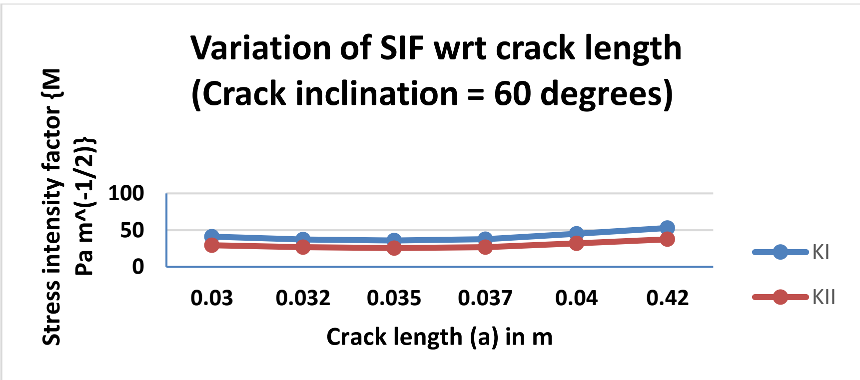

Fig. 4c. variation of SIF w.r.t. crack length at 60 degree

The change in the Stress Intensity Factor (SIF) with crack length at crack angle of 60° is shown in Fig. 4c. As with the other figures, the crack length (labeled as a) appears on the x-axis, and the SIF values as obtained under the Mode I and Mode II loads appear on the y-axis. As shown in Figure 4c, when the crack length is increased, the SIF increases, and both KI and KII take on an obvious upward trend. By 60° this increment on the SIF is more evident than at the lower angles (30° and 45°), especially Mode II (KII). That implies that the material would undergo a greater shear stress when it is at an angle of 60°, and as the crack increases, the shear contribution becomes even bigger than it was on Mode I. A higher value of KII is an indication of the increased role played by the shear stresses in the process of crack propagation in the mixed-mode loading regime. Even in this instance, the very correlation between crack length and SIF remains non-linear, with both KI and KII rising at a proliferative rate as a portion of increasing crack length. Nonetheless, the gradient of KII seems to be higher than the gradient of KI, which means that the shear aspect of the loading situation has a stronger impact on the fracture behavior of the material at larger crack angles (e.g., a 60 angle of crack). This finding points to the (mixed-mode) fracture mechanics, which are highly complex in that the opening (Mode I) as well as shearing (Mode II) stresses both interact as the crack extends, thus enabling a crack to propagate more easily under larger stresses. In general, Figure 4c adds further support to the premise that the crack angle plays a large role in dictating the stress intensity factors and the factors' dependence on a varying crack length.

Variation in Critical Stress Intensity Factor (Fracture Toughness)

Fracture toughness has also been calculated as the stress intensity factor. In the analysis formulation process, the brittleness material assumption is made, and the linear elasticity assumption is made. The Fig. 5 will be a representation of the variation of critical SIF against crack length at different orientations. Contrary to the theories, a reducing pattern in the values of Kic has been noticed with the growing length of the crack. The difference could be as a result of non-linearity that occurred at longer crack lengths.

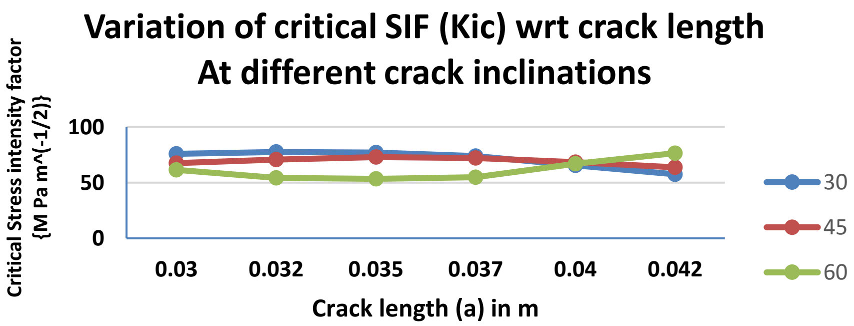

Fig. 5. Variation of critical SIF w.r.t. crack length

Figure 5 illustrates that the critical Stress Intensity Factor (SIF), KIc, varies with crack length (a) under various loading conditions. On the x-axis, the length of the crack is indicated, and on the y-axis, the critical SIF values are indicated, that is used as a measure of material fracture toughness. One of the main points of the plot that is to be emphasized is that with an increase in the length of the crack, the critical KIc diminishes, on average, at all crack angles (30^o, 45^o and 60^o). The decrease indicates that the prolonged cracks minimise the toughness of materials to fracture in a mixed loading mode. A higher critical KIc, which means a greater fracture resistance, is achieved at shorter crack lengths, whereas the larger the crack length, the weaker the contact becomes for the crack propagation. Out of the various crack angles, one can see that KIc values differentials are maximum at 30^o and tend to reduce progressively as the angle of the crack increases to 45° and 60°. This tendency proves how the angle of loading influences the fracture toughness of the material. The crack angles lower (e.g., 30°C) are more difficult to fracture because there is probably a dominating component of tensile stress (Mode I). In comparison, the shear stress (Mode II) value increases with an increase in crack angle, and so a higher angle (such as 60^o) will lower the material toughness. The behaviour of the mixed-mode fractures is very complex in that the crack length dependence on KIc is nonlinear in direction, as is also its dependence on the angle of the crack. The results play a very important role in future predictions of material behavior with a complex mixed-mode loading and crack-length insensitive loading conditions, which are used in the engineering design of components with better fracture resistance.

Von-Mises Stress distribution around the crack tip

Fig. 6 and Fig. 7 show the von-mises stress distribution around the crack tip at 45 degrees, having a crack length of 35mm, and 60 degrees, having a crack length of 42mm, respectively.

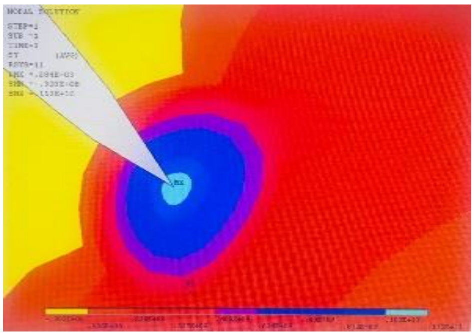

Fig. 6. von-mises stress distribution at 45^o

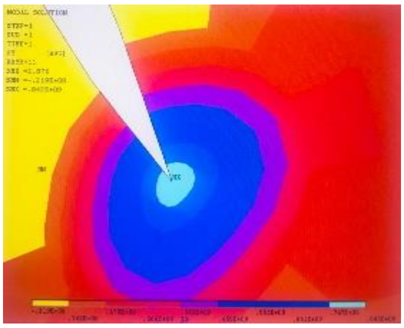

Fig. 7. von-mises stress distribution at 60^o

Figure 6 shows the Von-Mises stress distribution at 45^o crack angle. The stress contours around the crack tip indicate the presence of concentrations of stresses near the crack tip, especially around the notch immediately in front of the crack tip. The pattern is a sign of local level plastic strain under mixed-mode loadings involving tensile (Mode I) or shear (Mode II) stress and shear stress. The intensity of stress is asymmetrical along the crack; you are near the crack tip trace, but along the direction of crack propagation, indicating maximum shear contribution along this direction. It can also be noticed in the distribution that there is a gradual decay of stress with increasing distance to the crack tip, which helps to prove that stress is concentrated in the nearby area to the crack. Figure 7 shows the Von-Mises stress contours with a 60º crack angle. The displacement field at the crack tip is a stress concentration compared to the 45º case with wider stress areas far away from the crack tip. The dispersion corresponds to greater shear stress component (Mode II dominance) at this angle, and this alters the distribution of stress as compared to lower angles. The magnitudes of maximum stress are a little displaced toward the crack propagation line, and this demonstrates the interaction of tensile and shear modes under a mixed-mode loading condition. Conducting the comparison between Figure 6 and Figure 7, it can be stated that the crack angle has a significant influence on the distribution of Von-Mises stress. The stress field is lower at 45 2C, indicating a greater overall effect of tensile and shear stress. At 60, the stress field is more diffusive, and it depicts increased contribution of shear stresses.

Table 5: Analysis and trends for variations in the Stress Intensity Factor (SIF)

Crack Length (mm)	KI (30°)	KII (30°)	KI (45°)	KII (45°)	KI (60°)	KII (60°)	Critical SIF (30°)	Critical SIF (45°)	Critical SIF (60°)
30	15.2	8.3	16.8	9.6	18.4	12.1	28.5	27.8	26.9
31	15.8	8.7	17.5	10.2	19.1	12.7	28.2	27.5	26.7
32	16.5	9.2	18.3	10.9	20.0	13.4	27.8	27.2	26.4
33	17.3	9.8	19.2	11.7	20.9	14.2	27.4	27.0	26.1
34	18.1	10.5	20.1	12.5	21.8	15.0	27.1	26.7	25.9
35	18.8	11.0	21.0	13.3	22.6	15.9	26.8	26.5	25.6
36	18.2	10.6	20.5	12.9	23.1	16.3	26.4	26.1	25.3
37	17.5	10.1	19.8	12.3	23.5	16.8	26.0	25.7	25.0
38	16.8	9.6	19.2	11.7	24.0	17.3	25.7	25.4	24.8
39	16.0	9.0	18.5	11.1	24.4	17.8	25.3	25.1	24.6

Table 5 offers some information on the variations of Stress Intensity Factors (SIFs) with the variance of the length of a crack and crack angle when the crack is under mixed-mode load conditions is provided. The SIFs of tensile stress (KI) and shear stress (KII) are tabulated at crack angles of 30º, 45º and 60º. Also, maximum decisive values of SIF of each angle are evidence of the fact where the anxiety of the material starts fracturing, where there is a crack propagation. The table reflects the variation of SIF and crack behavior as length and angle change with the combined role of tensile and shear stresses. Both KI and KII also tend to become bigger at all crack angles as the length of the crack is extended to 39mm. This is because this trend shows that longer cracks increase stress concentration around the crack tip, further increasing the possibility of the crack propagating. But the increment is higher in the case of KI as compared to KII, which shows how tensile stresses are more than shear stresses as the length of the crack increases. Checking KI at 30º angle of crack, the values are relatively low compared to the angles at 45º, 60º, and 90º but the values of KII are moderate. The distribution represents the addition of equal amounts of tensile and shear stresses in this direction. At 30º the SIF critical values also decrease progressively with increasing crack length, with values of 28.5- 25.3, which denotes steadiness in material hardness with the duration of crack expansion. The values of KI and KII are higher at 45^o rather than 30^o in the case of crack angle 45^o, which further indicates that the mixed-mode loading plays a major role at the 45 ° angle compared to the loading at the 30^o angle. The critical SIFs are relatively addressed (ranging between 27.8 and 25.1), indicating that the fracture behavior of the material is less subject to any variation of the crack length in this angle. This points out the role of interactivity between tensile stress and shear stress in the determination of crack propagation. Angle of crack 60 has the highest KI of all the angles with large numbers of KII, thus meaning that at this angle, shear stresses dominate in the crack. The factors of stress intensity have a wider dispersion, which denotes the increased role played by shear stresses. The explicit values of SIF (26.9 to 24.6) reduce slightly with the crack length, depicting the affected interaction between the tensile and shear stress in the process of modifying the fracture resistance of the material. The behaviour of this angle displays the significance of shear-driving conditions in the analysis of mixed-mode fractures.

V. Conclusion

This study successfully determined the fracture toughness of mild steel under mixed-mode loading conditions by integrating experimental testing and finite element analysis. The test specimen of the experimental setup was testing of rectangular plates of mild steel with inclined through-edge cracks to ascertain the critical stress levels. Based on these experimental results, modelling was established in ANSYS, and the stress intensity factors (SIFs) of the Mode I (tensile) and Mode II (shear) loading were computed. The fracture toughness, represented as the critical stress intensity factor (KIc), was determined using the maximum hoop stress theory and found to range between 53 and 78 MPa/m^{½}. The research also explored the effects of crack length and crack inclination angle on the stress intensity factors. The findings highlight that both crack geometry and loading conditions significantly influence the material's fracture behaviour. Longer crack lengths and steeper crack angles generally resulted in higher stress intensities, demonstrating the critical interplay between these parameters. The parametric study provided a deeper understanding of how mixed-mode loading impacts fracture propagation in mild steel, contributing to predictive modelling and material design under similar conditions. By combining experimental and computational approaches, the study ensured robust and comprehensive results, with experimental data validating the finite element simulations. This methodology enhances the reliability of fracture toughness evaluation, providing a valuable tool for assessing material performance in structural applications subjected to complex loading scenarios. These findings have practical implications for designing mild steel components to resist failure under mixed-mode conditions, ensuring safety and durability in engineering applications.

Conflict of Interest:

There was no relevant conflict of interest regarding this paper.

References

I. Aliha, M. R. M. and A. Bahmani, "Rock fracture toughness study under mixed mode I/III loading," *Rock Mechanics and Rock Engineering*, vol. 50, no. 7, pp. 1739–1751, 2017.

II. Aliha, M. R. M. and H. Saghaf, "The effects of thickness and Poisson's ratio on 3D mixed-mode fracture," *Engineering Fracture Mechanics*, vol. 98, pp. 15–28, 2013.

III. Atkins, G. and R. E. Maietta, "Mixed mode fracture toughness for a composite material," *Composites Science and Technology*, vol. 15, pp. 319–330, 1982.

IV. Barsom, J. M. and S. T. Rolfe, *Fracture and Fatigue Control in Structures: Applications of Fracture Mechanics*. Oxford, U.K.: Butterworth-Heinemann, 1999.

V. Carpinteri, A., "Stress intensity factors for cracks emanating from stiffened panels," *International Journal of Fracture*, vol. 68, no. 4, pp. 389–398, 1994.

VI. Chowdhury, M. M. et al., "Improving mixed-mode fracture properties of concrete reinforced with macrosynthetic plastic fibers: Experimental and numerical investigation," *Buildings*, vol. 14, no. 8, pp. 2543, Aug. 2024, doi:10.3390/buildings14082543.

VII. Fagerholt, E., C. Dørum, T. Børvik, H. I. Laukli, and O. S. Hopperstad, "Experimental and numerical investigation of fracture in a cast aluminium alloy," *International Journal of Solids and Structures*, vol. 47, no. 24, pp. 3352–3365, 2010.

VIII. Guo, W., H. Dong, and Z. Yang, "Experimental investigation of thickness effects on mixed-mode I/II fracture of an aluminum alloy," *arXiv preprint arXiv:0807.1577v2*, 2008.

IX. Hossain, R., L. R. Wilson, and C. Tang, "Advanced mixed-mode I/II fracture analysis of polymer-based adhesives," *Polym. Eng. Sci.*, vol. 64, no. 1, pp. 15–26, Jan. 2024. 10.1002/pen.26045.

X. Kamat, S. V. and J. P. Hirth, "Mixed mode I/II fracture toughness of 2034 aluminum alloys," *Acta Materialia*, vol. 44, no. 1, pp. 201–208, 1996.

XI. Li, J., X.-B. Zhang, and N. Recho, "J–Mp based criteria for bifurcation assessment of a crack in elastic–plastic materials under mixed mode I–II loading," *Engineering Fracture Mechanics*, vol. 71, no. 3, pp. 329–343, 2004.

XII. Matvienko, Y. G., A. S. Chernyatin, I. A. Razumovsky, H. J. Shi, and Z. X. Wang, "The effect of thickness on components of the nonsingular T-stress under mixed mode loading," in *Proc. of the 13th Int. Conf. on Fracture*, Beijing, China, 2013.

XIII. Miao, X.-T., Q. Yu, C.-Y. Zhou, J. Li, Y.-Z. Wang, and X.-H. He, "Experimental and numerical investigation on fracture behavior of CTS specimen under I–II mixed mode loading," *European Journal of Mechanics - A/Solids*, vol. 72, pp. 235–244, 2018.

XIV. Mu, M. Y., G. Z. Wang, S. T. Tu, and F. Z. Xuan, "Three-dimensional analyses of in-plane and out-of-plane crack-tip constraint characterization for fracture specimens," *Fatigue and Fracture of Engineering Materials and Structures*, vol. 39, no. 12, pp. 1461–1476, 2016.

XV. Nasrnia, M. and F. H. Aboutalebi, "Experimental investigation and numerical simulations of U-notch specimens under mixed mode loading by the conventional and extended finite element methods," *Archive of Applied Mechanics*, 2018. 10.1007/s00419-018-1381-y.

XVI. Nguyen, H. T., S. M. Nguyen, and J. D. Kim, "Evaluation of mixed-mode fracture properties of aerospace-grade aluminum alloys under varying thermal conditions," *J. Mater. Eng. Perform.*, vol. 32, no. 2, pp. 225–234, Feb. 2023. 10.1007/s11665-022-3015-8.

XVII. Pearce, G. M., C. Tao, Y. H. E. Quek, and N. T. Chowdhury, "A modified Arcan test for mixed-mode loading of bolted joints in composite structures," *Composite Structures*, vol. 187, pp. 203–211, 2018.

XVIII. Pirondi, A. and C. D. Donne, "Characterisation of ductile mixed-mode fracture with the crack-tip displacement vector," *Engineering Fracture Mechanics*, vol. 68, no. 12, pp. 1385–1400, 2001.

XIX. Ramesh, K. T. and R. S. Barsoum, "Dynamic fracture toughness evaluation of materials," *Journal of Mechanics and Physics of Solids*, vol. 38, pp. 377–393, 1990.

XX. Rice, J. R., "A path independent integral and the approximate analysis of strain concentration by notches and cracks," *Journal of Applied Mechanics*, vol. 35, pp. 379–386, 1968.

XXI. Rossi, P., T. Ricci, and M. Leone, "Mixed-mode fracture behavior of carbon-fiber-reinforced composites using the edge crack torsion method," *Compos. Sci. Technol.*, vol. 231, pp. 108528, May 2023, 10.1016/j.compscitech.2023.108528.

XXII. Seitl, S., P. Hutar, T. E. García, and A. Fernández-Canteli, "Experimental and numerical analysis of in- and out-of-plane constraint effects on fracture parameters: aluminium alloy 2024," *Applied Computational Mechanics*, vol. 7, pp. 53–64, 2013.

XXIII. Tada, H., P. Paris, and G. Irwin, *The Stress Analysis of Cracks Handbook*, 3rd ed. New York: ASME Press, 2000.

XXIV. Takahashi, J. and Y. Kawaguchi, "Recent advances in computational modeling of mixed-mode fracture mechanics in brittle materials," *Theor. Appl. Fract. Mech.*, vol. 121, pp. 103779, Mar. 2023, 10.1016/j.tafmec.2023.103779.\

XXV. Zhang, S., W. Guo, H. Li, and Y. Deng, "Experimental investigation of three-dimensional mixed-mode fracture of a titanium alloy at room and elevated temperatures," *Science China Technological Sciences*, vol. 54, no. 10, p. 2760, 2011